URTeC: 1521

Pozo D-129 Formation: The Case of a Recent Shale Oil Discovery in a Lacustrine Source Rock in El Huemul Field, Golfo San Jorge Basin, Southern Argentina

P. A. Caprioglio*[1], G. Jarque[1], M. Irigoyen[1], G. Maiztegui[1], N. Luz[1], A. D'Agostino[1], M. Casal[1], D. Villalba[2], H.J. Villar[2], 1. Sinopec Argentina Exploration and Production, Inc., 2. GeoLab Sur S.A.

This paper was prepared for presentation at the Latin America Unconventional Resources Technology Conference held online on 16-18 November 2020.

Abstract

Since the discovery of conventional oil in 1907, the Golfo San Jorge Basin (GSJB) has become into one of the most prolific hydrocarbon basins of Argentina, having an estimated areal extension of 180,000 km^2. To this date, scarce information has been publicly released about unconventional exploration on its main hydrocarbon source rock, the lacustrine, Lower Cretaceous Pozo D-129 Formation (D129 Fm.).

The evaluation of the D129 Fm. for unconventional opportunities in El Huemul Field (EH) started in year 2013 and led to a recent shale oil discovery in well EHa-4301, which tested oil not only during completion but also began production under regular field operation conditions. Furthermore, shale-oil occurrence was also observed in well EH-4324.

To understand organic richness distribution, kerogen type, hydrocarbon potential and thermal maturity windows of the D129 Fm. source rock in the area, 411 cutting samples obtained from 19 wells distributed along operated concessions were submitted to typical geochemical analysis that included TOC, programmed pyrolysis and organic petrography. Results show that current organic contents corresponding to the deep present structural position of the EH Field attain TOC values higher than 3% with the tightest cloud ranging between 0.8 and 2%. Type I lacustrine kerogen is predominant in the deepest facies of D129 Fm., while enrichment with Type III stands out in the transition to terrestrial-influenced facies. Thermal maturity spans a wide range from marginal-early stages of the oil window to late oil and transition to the gas-condensate stages.

Oils obtained from the D129 Fm. source rock in the EH Field show good states of preservation, contrary to conventional oils in the area, which typically depict evidences of biodegradation, rejuvenation and mixing processes that involve renewed migration pulses. In terms of physical characteristics, the produced shale oil exhibits API gravities around 44°, reflecting an outstanding quality in comparison with average conventional hydrocarbons of the basin.

In terms of potential, the D129 Fm. Upper Section constitutes a shale-oil target having an average thickness of 250 m. Next, the D129 Fm. Middle Section represents a hybrid system (interbedding of shale and tight) with potential for oil and gas production. Last, the D129 Fm. Lower Section seems to integrate two unconventional targets having different potential and is expected to be within the gas window. Adding up all three sections, the total oil window may even exceed 700 m of thickness for potential hydrocarbon production.

Introduction

The analysis of the Pozo D-129 Formation (D129 Fm.), main source rock of the Golfo San Jorge Basin (GSJB), started as early as year 2013 in El Huemul Field (EH) looking for unconventional opportunities. During the first stage, permeable reservoir intervals close to the top of D129 Fm. were tested to assess the nature of hydrocarbons together with the distribution and amount of CO_2. Moreover, attention was given to establish the thermal maturity status of these hydrocarbons and their relationship with their source facies.

A second stage focused on testing the unconventional shale play within the upper section of D129 Fm. source rock was afterwards performed. Three wells (EHa-4301, EH-4167, EH-4324), originally targeting only conventional reservoirs, were extended to drill the upper section of D129 Fm. These wells allowed to address several aspects of the new play such as: mechanical issues including rate of penetration; source rock, rock and hydrocarbon samples collection; logging data acquisition; target selection criteria; fracture design; real mechanical behavior during fracture jobs; further analysis of CO_2 distribution; hydrocarbon testing; among others.

This second stage constituted a milestone in the history of D129 Fm. in the area: a *Shale Oil, Unconventional Play, was Discovered by well EHa-4301*. The well tested oil during completion and also began producing under regular field operation conditions. Furthermore, well EHa-4301 also proved that it is mechanically possible to perform fractures on D129 Fm. shale. *Fluid samples compatible with shale-oil characteristics were also obtained from well EH-4324*. In another key outcome of this stage, both wells proved very low CO_2 content in the sampled shale intervals.

A third stage, involved a massive characterization process of D129 Fm. within EH Field that included: seismic, geological and paleoenvironmental interpretations; velocity analysis and generation of depth and thickness maps; geochemical characterization of D129 Fm. sections including organic richness distribution, kerogen typing by programmed pyrolysis (SR analyzer instrument) and organic petrography, thermal maturity assessment, and typing of hydrocarbon fluids; lithofacies and electrofacies definition; mud-logging chromatographic ratios to evaluate native/migrated nature of hydrocarbons; analysis of low coherency seismic vertical zones –“gas chimneys”- and igneous dikes presence along the field together with the associated CO_2 risk of affected areas; evaluation of potential exploratory volumes; among others.

The overall thickness of D129 Fm. can be even higher than 800 m, but the most promising section for a shale oil play is the Upper Section with a thickness ranging between 200 and 300 m and homogeneous shale lithology, that it is expected to be within the oil window. On the other hand, the other two sections can present a 500 m total thickness of interbedding of shale and more permeable lithologies, with a significantly higher thermal maturity that include the late oil and gas windows, in a possible hybrid resource system. In this framework, the present contribution will focus on the characterization of the D129 Fm. source rock and its potentiality as an unconventional resource system, describing the geochemical patterns of the organic rich shales and the associated hydrocarbons.

Geological Framework

The Golfo San Jorge Basin (GSJB) is located in southern Argentina, covering 180,000 km^2 of the Chubut and Santa Cruz provinces. After the discovery of commercial oil in 1907 it became the most prolific hydrocarbon basin in the country. The Somuncurá Massif to the north and the Deseado Massif to the south limit the onshore sector of GSJB. Westward it is limited by the Rio Mayo High and to the east by the Malvinas Arch (Urien *et al.*, 1981), where it continues offshore in the Atlantic Ocean. The study area comprises the 600 km^2 of the EH Field in Sinopec Argentina E&P concessions. (Figure 1).

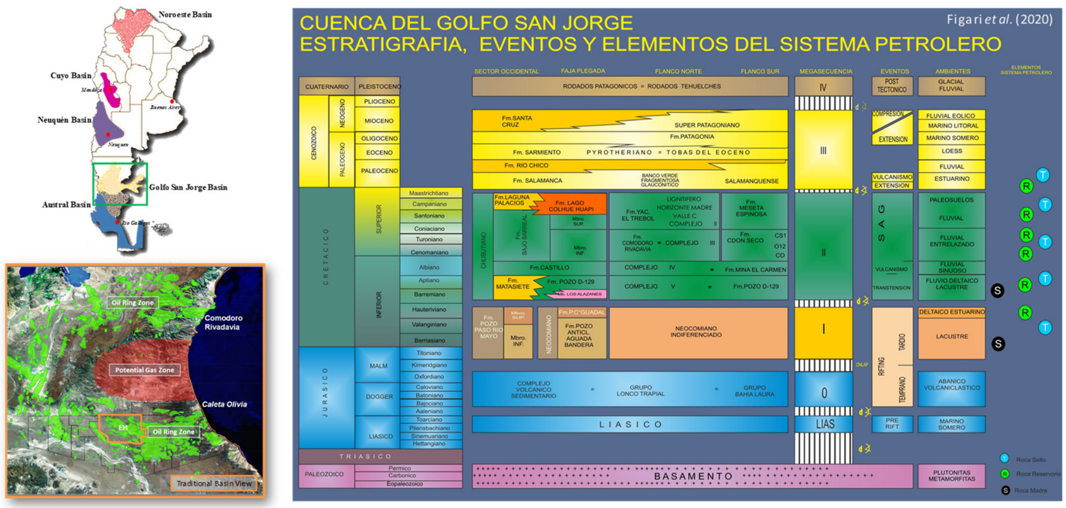

Figure 1. Location map of Golfo San Jorge Basin in Argentina and position of El Huemul Field within the Basin indicated in bold orange. Stratigraphic chart according to Figari *et al.* (2020).

The San Jorge is an intracratonic extensional basin, formed as a response to the breakup of Gondwana supercontinent (Dingle *et al.,* 1983; Fitzgerald *et al.*, 1990; Figari *et al.*, 1999, 2002) mainly during the Jurassic and Early Cretaceous. Volcaniclastic deposits of Bahia Laura Group and older crystalline rocks filled the generated space and represents the economic basement of the basin. The regional basin structural configuration is mainly defined by the W-E and NW-SE faulting trends (Fitzgerald et at. 1990). In the central–west area, the tertiary Andean orogeny (Miocene) originated the transpressive San Bernardo Fold Belt lineament with NNW - SSE orientation, interrupting the normal regional faulting pattern mentioned before.

Although the western part of the basin was open to marine influence, represented by Las Heras Group known as "Neocomiano" (Figari *et al.,* 1997), most of the Mesozoic sedimentary column corresponds to terrigenous deposits: fluvial, fluvial – lacustrine (with generation of small deltaic systems) and fine lacustrine facies. These sequences can be divided into different continental deposits related to the syn-rift stage (Triassic – Middle Jurassic), the late syn-rift (Upper Jurassic – Lower Cretaceous), beginning of the thermal subsidence (Lower Cretaceous) and late thermal subsidence deposits (Upper Cretaceous – Paleocene). A set of cretaceous deposits lies unconformable above the Neocomian and corresponds to the Chubut Group. The first deposits related to early thermal subsidence correspond to D129 Fm. (Upper Hauterivian – Lower Aptian) with variable thickness depending on its position and representing the main source rock of the basin.

The D129 Fm. sedimentation took place in Hauterivian – Aptian times (Archangelsky and Seiler, 1980) in a saline-alkaline, well-stratified lake with bottom waters depleted of oxygen under semi-arid climate conditions (Van Nieuwenuise and Ormiston, 1989; Paredes *et al.*, 2007). Its lithology is dominated by a wide variety of clastic rocks (mainly organic-rich black shales) with sizeable amounts of pyroclastic components due to its sedimentation during the early evolution stages of the Andean Ranges. Carbonate rocks are volumetrically small and include limestones and oolitic limestones (Clavijo, 1986; Fitzgerald *et al.*, 1990; Hechem and Strelkov, 2002). Figari *et al.* (2002) defined six regional sedimentary facies for the D129 Fm. Pyroclastic facies (proximal and distal) predominate to the west; coarse clastic and litoral-distal clastic facies are common in the basin margins (North and South Flanks); shallow and deep lacustrine fine-grained facies prevail in the basin center (Figure 2).

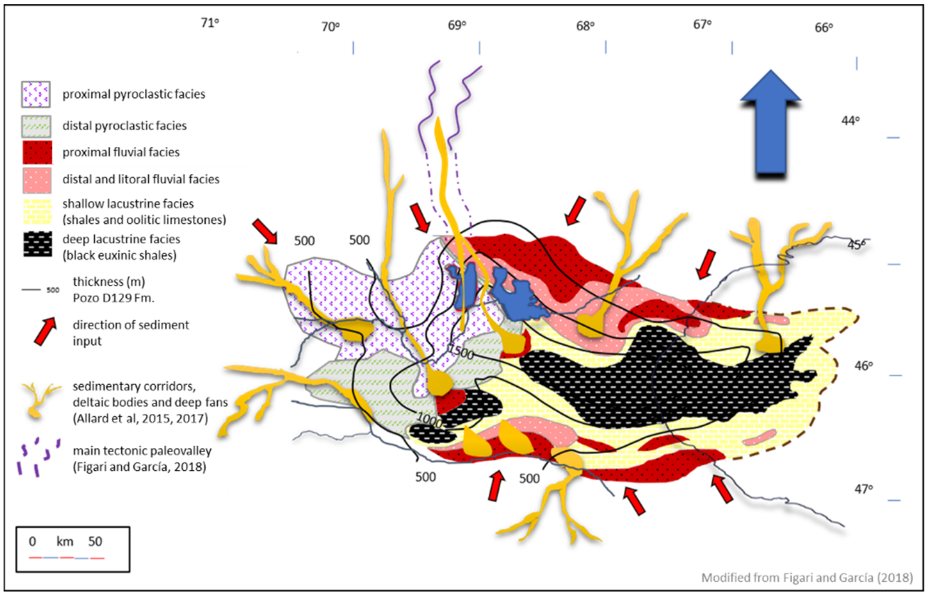

Figure 2. Regional facies model for the D129 Fm. Modified from Figari and García, 2018.

During the Albian, Mina del Carmen Fm. was deposited (towards the center and south-center of the basin) and its lateral equivalent Castillo Fm. (west and south-west), mainly represented by large volcaniclastic and fluvial channel deposits. Throughout the Upper Cretaceous, the Bajo Barreal Fm. and equivalents were deposited (Comodoro Rivadavia Fm. in the north and Cañadon Seco Fm. in the south-southeast) where a progressive decrease of pyroclastic material occurred to the top. The sedimentary column ends with Cenozoic deposits of the Salamanca, Rio Chico, Patagonia and Santa Cruz Fms. (Uppermost Cretaceous – Neogene; Fitzgerald *et al.,* 1990).

<u>D129 Fm. Source Rock</u>

Different publications have thoroughly documented the stratigraphic and geochemical characteristics of the D129 Fm. lacustrine shale as the predominant source rock in the basin and its associated petroleum accumulations (Lesta, 1968; Van Niewenhuise & Ormiston, 1989; Yllañez *et al.*, 1989; Villar *et al.,* 1996; Figari *et al.*, 1999, 2002; Uliana *et al.*, 1999; Rodriguez and Littke, 2001; Sylwan *et al.*, 2008; Legarreta and Villar, 2011; Basile *et al.*, 2014). The conventional reservoirs have been integrated by terrestrial-fluvial systems: Mina del Carmen and Castillo Fms. in the Albian, Bajo Barreal Fm. in the Upper Cretaceous, and minor Tertiary units. As much as 95% of the hydrocarbon reserves in GSJB are suggested to have been originated in the D129 Fm. source rock (Sylwan *et al.,* 2008).

The D129 Fm. has been typically described as an organic rich shale, in which high-quality, oil-prone, algal-amorphous Type I kerogen prevails; enrichment with land plant derived type III kerogen can occur under terrestrially influenced facies. Present-day TOC values typically range from 0.8 to 2-3%, with occasional peaks of 5.5-7%; hydrogen index (HI) data of around 500 mg/g, or sporadically higher, are typical of the better and low-mature organic facies. The "Cuello Pelítico" term introduced by Basile *et al.* (2014) represents a specific interval in the upper section that displays the richest organic content. A recent paper by Utgé *et al.* (2014) has discussed the geochemical and mineralogical pattern for D129 Fm. to be considered as a potential unconventional resource at a basin scale.

D129 Fm. Sequences

Four seismic horizons have been defined within the D129 Fm. and interpreted across the EH Field (Figure 3a). They are discriminated by a strong character and allowed the delineation of three seismic sequences in accordance with the observed lithological properties and the associated paleoenvironmental implications. Details regarding this lithological characterization of D129 Fm. will be published elsewhere. Additionally, these sequences are consistent with the D129 Fm. regional interpretation of Stach and Ansa (2014) in the South Flank (Figure 3b).

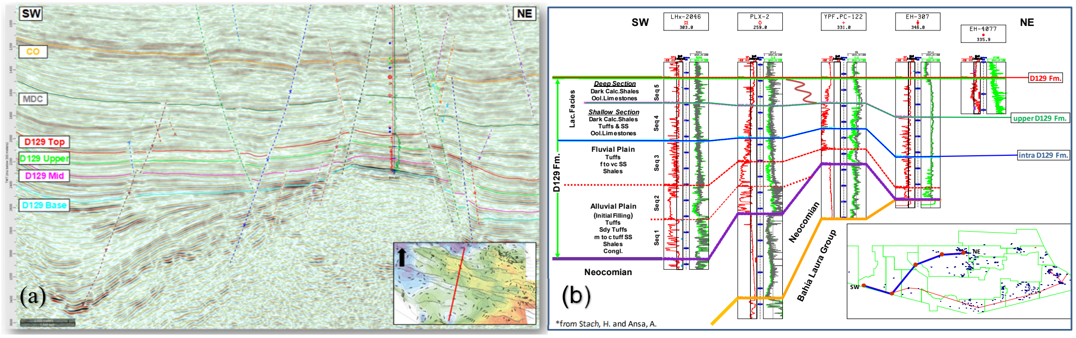

Figure 3. (a) SW-NE seismic section through EH Field. (b) Regional sequences interpreted by Stach and Ansa (2014).

The *D129 Fm. Upper Section,* defined between the D129 Fm. Top and the "D129 Upper" horizon, is associated with deep facies of the paleolake; the *D129 Fm. Middle Section*, between the "D129 Upper" and "D129 Mid", is related to shallower lacustrine facies, presenting a frequent interbedding of permeable levels; the *D129 Fm. Lower Section*, between the "D129 Mid" and the base of D129 Fm., is characterized by the regional transition into fluvial and alluvial systems showing again the interbedding of shale and permeable levels.

D129 Fm. Source Rock Characterization in the study area

Thirteen wells from EH Field and six wells from neighbor areas that penetrated D129 Fm. source rock, were selected for geochemical assessment (Figure 4), including a total of 360 cutting samples.

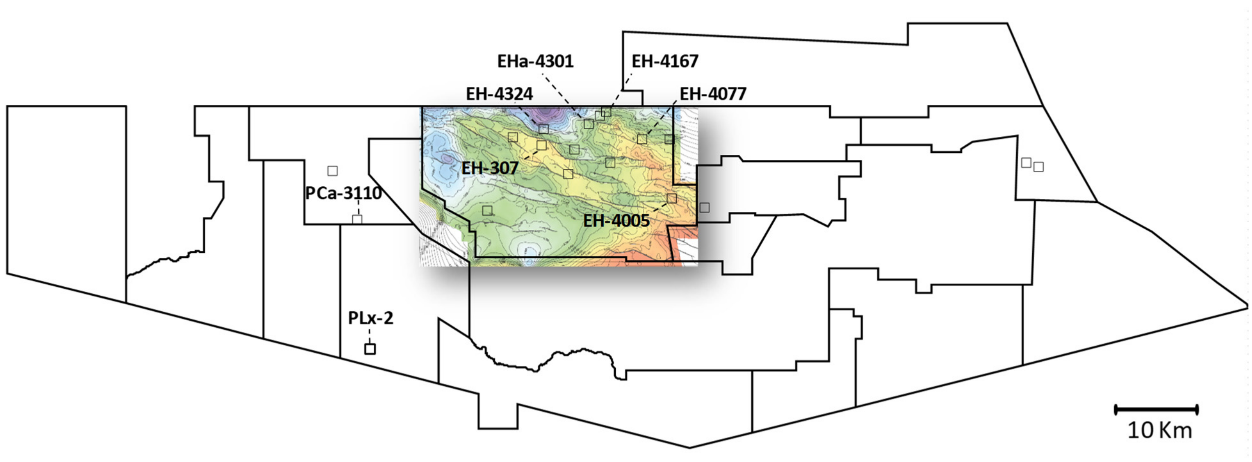

Figure 4. Concessions map showing the location of studied wells in the EH Field and neighbor areas (squares). Wells mentioned in the text are individually identified by mane. Structural map is shown at the top of D129 Fm.

The D129 Fm. in these nineteen wells shows a current TOC range of 0.8–2.0%, peaking over 3% with an average of 1.29%. The present generation potential (S1+S2 vs. TOC in Figure 5a) indicates moderate to good source rock characteristics (Figure 5a). Hydrocarbon potentiality is assumed to have been significantly higher before maturation. According to HI and OI values, the samples are interpreted to show trends pointing to Type I lacustrine and Type III terrestrial kerogens displaying low-moderate to advanced thermal maturity (Figure 5b), characteristics that where confirmed by organic petrography studies (see below).

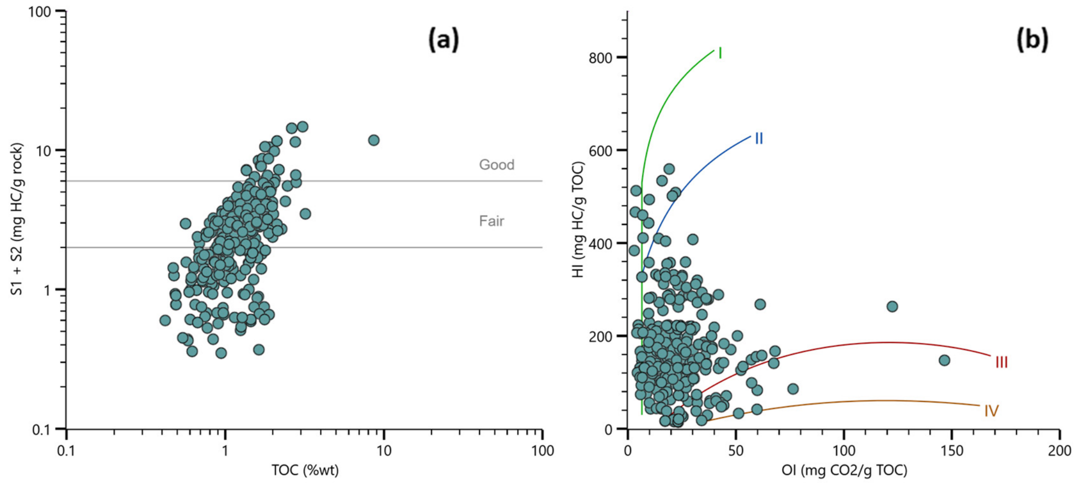

Figure 5. TOC and programmed pyrolysis data of the D129 Fm. cuttings set. (a) S1+S2 pyrolysis peaks vs. Total Organic Content (TOC%); (b) Hydrogen Index (HI) vs. Oxygen Index (OI) for kerogen typing.

Figures 6a and b show pyrolysis data for a selection of four wells displaying thermal maturities from early to late generation stages. Two of these wells, PL.x-2 and PC-3110, are outside of the EH Field and serve to illustrate the original organic characteristics of the Upper D129 Fm. before substantial conversion to hydrocarbons. Wells EH-4005 and EH-4324 represent mid and late maturity patterns in EH Field.

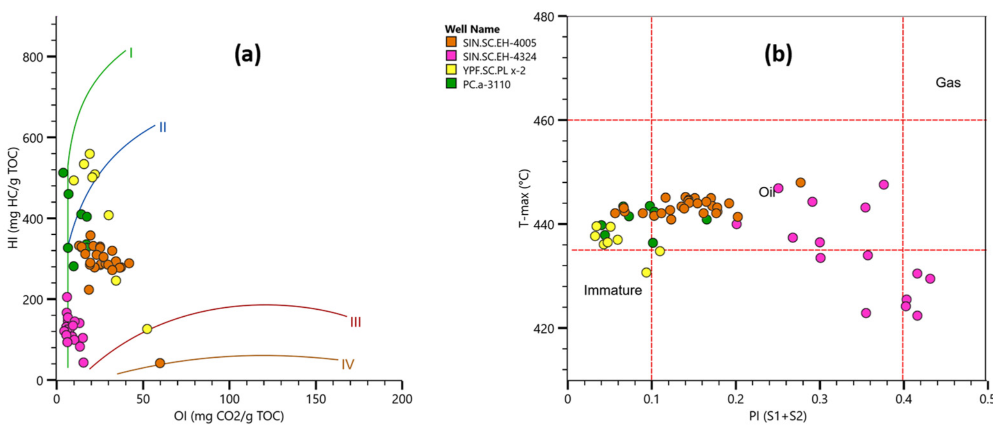

Figure 6. Programmed pyrolysis data on four selected wells with different thermal maturity of the Upper D129 Fm. (a) Hydrogen Index (HI) vs. Oxygen Index (OI) for kerogen typing. (b) Thermal maturity estimation from pyrolysis Tmax and Production Index (PI).

The shallower samples of PL.x-2 representing the Upper D129 Fm. (150 m section), have a vitrinite reflectance (Ro) of 0.60% and show HI values in the range 500-600 mg/g for the high-quality organic facies. Samples of PCa-3110, with a Ro averaging 0.74%, show a drop in HI to 300-500 mg/g interpreted as a result of kerogen conversion to hydrocarbons. This decreasing trend is continued in EH-4005 (average Ro: 0.82%) with a HI of about 300 mg/g, close to peak oil generation, and in EH-4324 (average Ro: 1.26%) at the end of the oil window, with a HI between 100 and 200 mg/g (Figure 6a). The overall data pictures the pyrolysis behavior and transformation to hydrocarbons of the dominantly Type I, D129 Fm. kerogen through the entire oil maturity window. The four-steps increase in the thermal maturity of D129 Fm. in the four key wells is reflected in the crossplot of Tmax vs. PI (Figure 6b).

Selected samples covering the D129 Fm. source rock from 14 wells have been analyzed with organic petrology methodology for organic matter typing (maceral composition). Results for the Upper and Middle D129 Fm. Sections are consistent with predominance of algal-amorphous, oil-prone, Type I kerogen, characteristic of the general knowledge at a basin scale (references in “D129 Fm. Source Rock” section), with minor but relevant (5 to 15%) presence of land-plants derived macerals of the vitrinite and inertinite type, occasionally associated to sporinite and cutinite. The scarce amount of Lower D129 Fm. beds available for study revealed a considerable increase in the contribution of terrestrial organic matter expressed as vitrinite and/or inertinite, implying a shift to Type III kerogen and mixed gas-oil hydrocarbon capacity. The diagram of Figure 7 portrays a detailed kerogen composition that includes several wells distributed along EH Field.

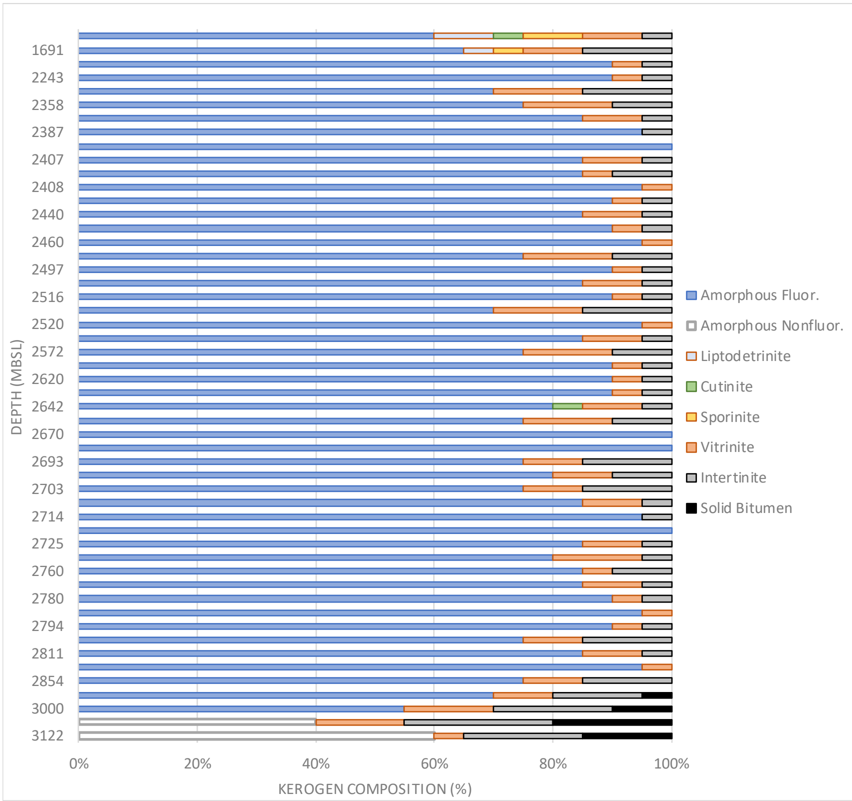

Figure 7. Summary of maceral composition vs. depth in 26 samples of 14 wells for the D129 Fm. in the study area. Vertical axis not in scale.

Thermal Maturity Analysis

The thermal maturity was assessed via vitrinite reflectance (Ro%) measurements in the same 14 wells studied for visual kerogen analysis. The obtained values cover the range 0.76-1.69% in a depth interval from ~2600 to 3500 m (MD). Slight variations on the thermal maturity trends are observed depending on the relative location of each well. Figure 8 shows the vitrinite reflectance measurements versus depth and the regression for three possible cases. The data trends split into two specific groups: one higher than the average tendency and other lower one, defined by the wells located on the basement high and by wells located on the basement low respectively (Figure 9). The well EH-4077 was excluded from the thermal analysis due to local alterations caused by magmatic intrusions. A feasible explanation to the split pattern is that, given the half-graben geometry of the basin, up to several hundred vertical meters can separate the D129 Fm. contact from the basement and so different thermal conductivities may exist. The structurally elevated areas of the basement in EH Field extend in SE to NW direction, where the thickness of the sediments lying between the base of the D129 Fm. and the basement is reduced even down to zero. However, in deeper positions these underlying sediments pile is thicker (up to 1000 m). This situation may impact differentially on the heat flow of both scenarios, due to the contrast of distinct thermal conductivities of sediments and the crystalline basement. Therefore, three differentiated trends (average/high/low; Figure 8) were defined, although further refinement may be required when more data becomes available.

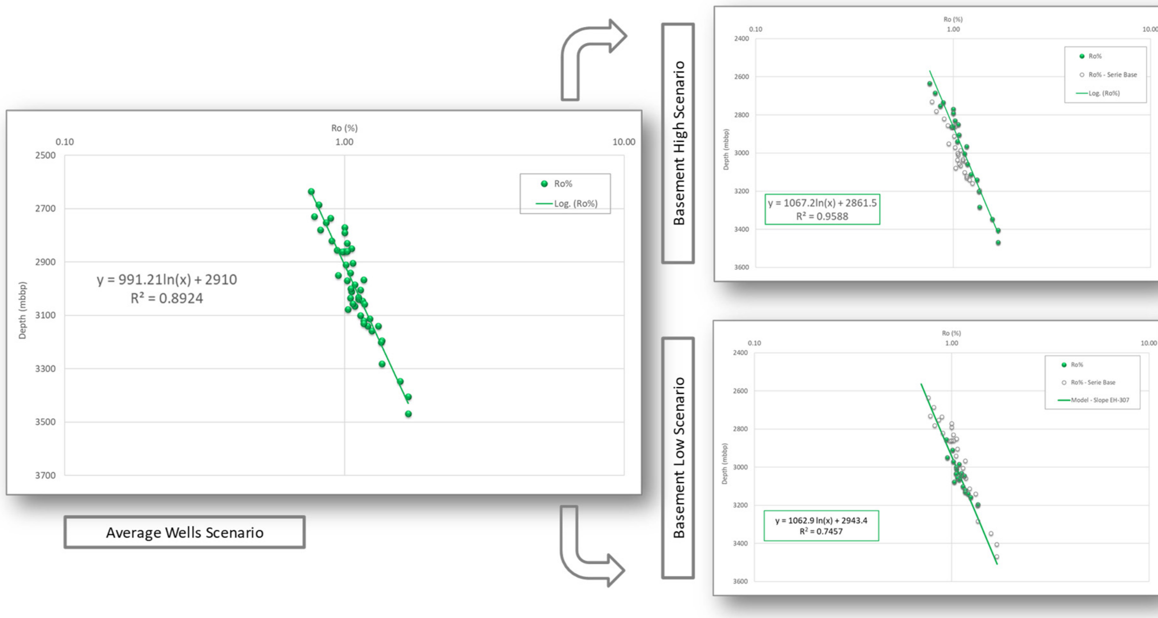

Figure 8. Depth vs. measured Ro (%) of the D129 Fm. to evaluate thermal maturity behaviors in three different scenarios within EH Field.

The general thermal framework is interpreted considering the average case scenario for the EH Field, which is a simplification, but it is useful for extrapolation to obtain simplified maps when dealing with general cases.

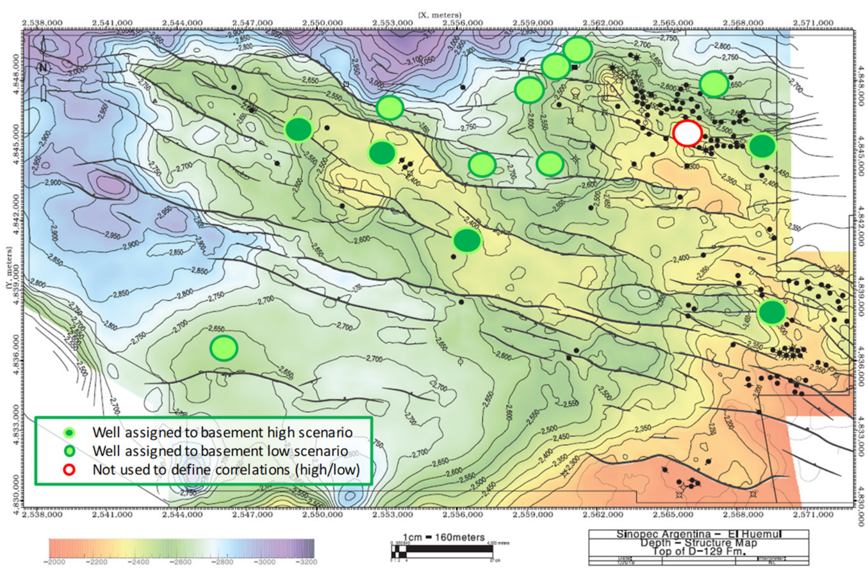

Figure 9. Structural map at the top of D129 Fm. in EH Field. Location of wells with vitrinite reflectance determinations referenced to high and low scenarios previously defined in Figure 8.

Interpreted maturity map at the top of D129 Fm. is shown in Figure 10a, referred to the average thermal scenario, compared to the thickness map (Figure 10b) in the oil window. Thus, the D129 Fm. Upper Section is expected to be within the oil generation window basically for the complete EH Field. Most of the areas that are shown in the gas window in Figure 10a are, in fact, within the oil window when the corrected "basement low scenario" is applied for those deeper sections of the field. The D129 Fm. Middle Section is to be found almost evenly distributed along the oil and gas windows while the Lower Section, on its turn, is expected to be essentially within the gas window.

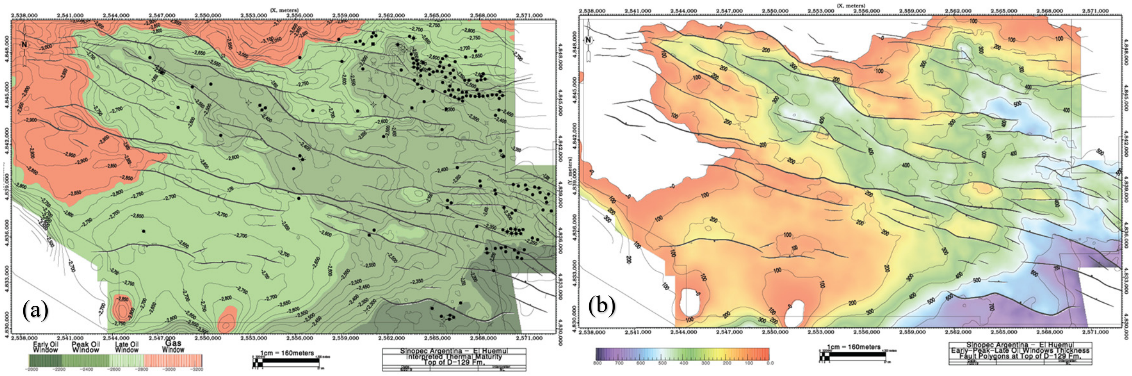

Figure 10. Maps of the EH Field for: (a) interpreted thermal maturity at the top of D129 Fm.; and (b) thickness of D129 Fm. where the source rock is expected within the oil generation window. Both maps are referred to the average-wells scenario.

EH-307: key exploration well

EH-307 is considered a key well since it is the only one of the very few which drilled through the complete D129 Fm., thus providing complete information for the three D129 Fm. sections (Figure 11).

As mentioned above, D129 Fm. Upper Section is mostly associated to rather deep facies of a lacustrine environment. It is shown by well EH-307 having 250 m of vertical thickness, mainly composed by black shales with minor intercalations of reworked tuffs and the eventual presence of oolitic limestones in its uppermost part. Even when the D129 Fm. Middle Section (300 m thick) is related to shallower lacustrine facies, the lithology is still mostly dominated by black shales with reworked tuffs and tuffaceous sandstones intercalations, but these are much more frequent than in the Upper Section. The Lower Section is framed within the regional transition into fluvial and alluvial systems. It still shows a dominant presence of organic rich black shales with reworked tuffs and tuffaceous sandstones interbedded, resulting in a higher "net-to-gross" with an associated thickness of 200 m.

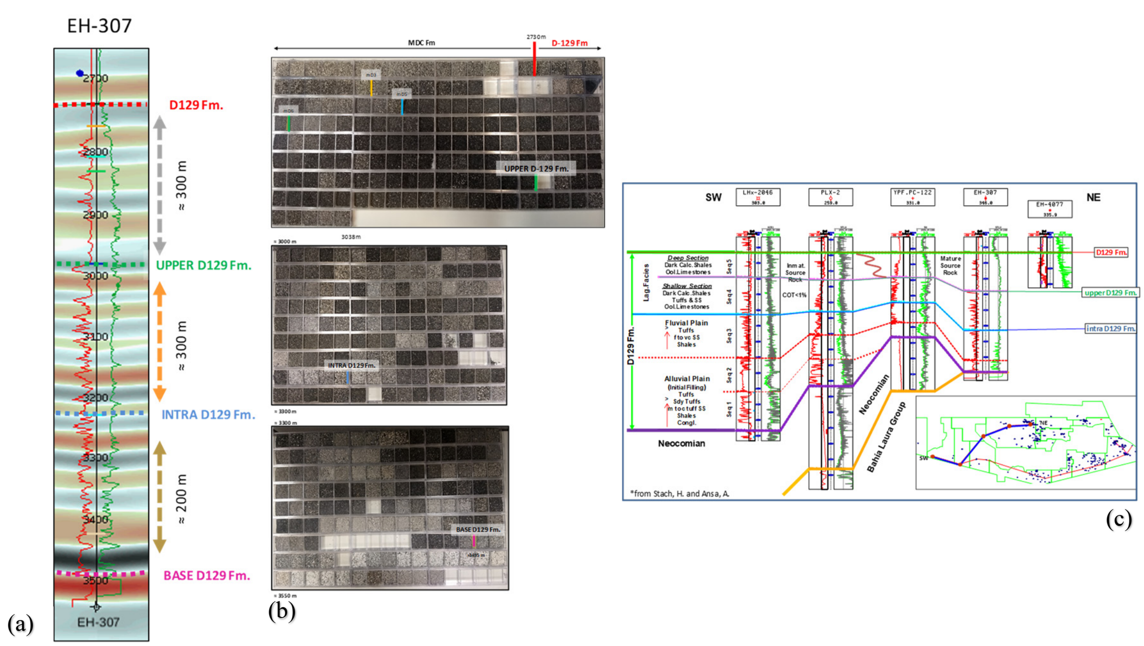

Figure 11. EH-307 well. (a) Seismic interpretation with over imposed well-logging. (b) Cutting samples outlook of Upper, Middle and Lower D129 Fm. Sections. (c) Reference cross-section including the EH-307 correlation.

The four deepest samples in Figure 7 correspond to the Lower Section in EH-307 and they show very different organic composition. Besides the higher inertinite content, the significant presence of solid bitumen (likely pyrobitumen) is in line with its high maturity.

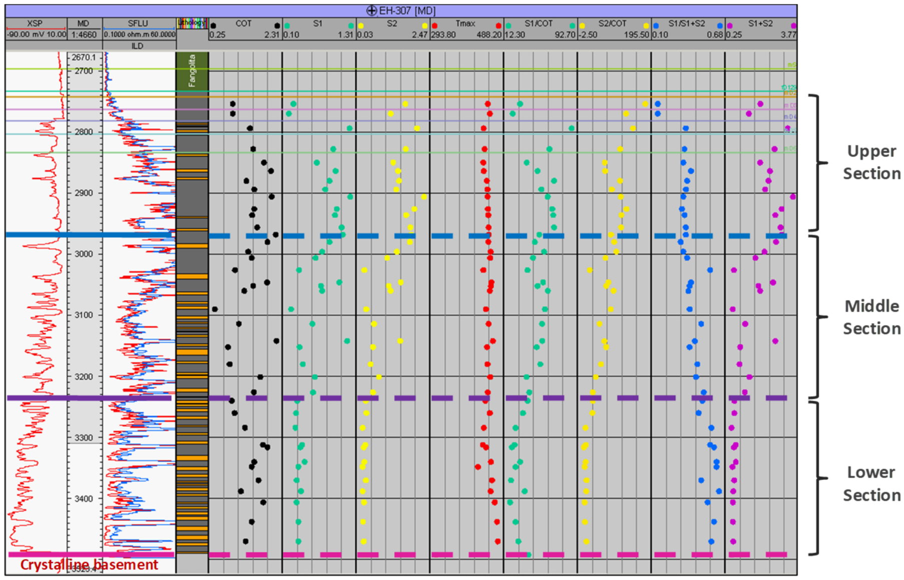

Figure 12. EH-307 Log tracks for D129 Fm.: SP, MD, Res, lithology, TOC, pyrolysis parameters (S1, S2, Tmax, S1/TOC, S2/TOC [HI], PI, S1+S2)

The associated EH-307 geochemical log shows the pyrolysis variations for the entire interval and delineates the sections differences. There is a clear trend from the Upper to the Lower Section mainly associated with the thermal maturity increment from 0.86 to 1.69 Ro%, where Tmax and PI relate each other from top to bottom (Figure 12).

The Upper section shows the richest characteristics, where despite moderate thermal maturity, it presents the highest average TOC and HI (S2/TOC). Even when TOC values are not particularly high, its distribution represents a continuous rich interval with no heterogeneous lean intercalations, in concordance with the previous cutting and kerogen description.

The Middle Section presents slightly lower average TOC values but scattered, indicating certain heterogeneity coherent with its associated shallower lacustrine facies. The HI (S2/TOC) is also somewhat lower and shows a clear decreasing trend from top to bottom due to the progression of the thermal maturity. Compared to the Upper Section, the OI (S3/TOC) is relatively higher, indicating certain lower quality kerogen intercalations.

When moving from the Middle to the Lower Section (Figure 12), S2 yields show a significant reduction parallel to a TOC increase, likely because of a lower original quality of the kerogen together with advanced thermal maturity, which results in the lowest HI values in this well (S2/TOC <50 mg/g). Consistently, the S1/TOC ratio is clearly low denoting an advanced hydrocarbon expulsion stage. This more limited hydrocarbon potential of the Lower Section when compared to the Middle and Upper Sections is in line with the documented increase in terrestrial input. Average values are summarized below:

Upper Section:

$\bar{S}_2 = 1.67$ mg/g
$\overline{TOC} = 1.57$ % wt
$\overline{HI} = 106$ mg/g

Middle Section:

$\bar{S}_2 = 0.87$ mg/g
$\overline{TOC} = 1.30$ % wt
$\overline{HI} = 67$ mg/g

Lower Section

$\bar{S}_2 = 0.29$ mg/g
$\overline{TOC} = 1.36$ % wt
$\overline{HI} = 21$ mg/g

To characterize the history and hydrocarbons potential of the Upper D129 Fm., a geochemical 1D model was performed on the EH-307 well. Given the complex thermal history of the basin (Rodriguez & Littke, 2001), a rifting model was applied where the current heat flow is 67 mw/m^2 at the base of the lithostratigraphic column. The simulated source rock is comprised of a mixture of “C-Aquiatic nonmarine (lacustrine)" and "D/E-Terrigenous terrestrial wax/resin" kerogens (Pepper and Corvi, 1995) with an average original TOC of 3% and an original HI of 573 mg/g. The kerogen kinetics simulation established the proper geochemical linkage between the original organic content and its conversion pathway until present residual kerogen (Figure 13a). The recreated burial history determined that the oil window for this upper section started at about 80 MY, with the beginning of the Meseta Espinosa Fm. deposition (Figure 13b). The transformation ratio (TR) reached 60-65% with a strong predominance of the oil phase over gas, with very optimistic volumetric estimations for retained and expelled oil, being each one higher than 10 mmstb/km^2/100m.

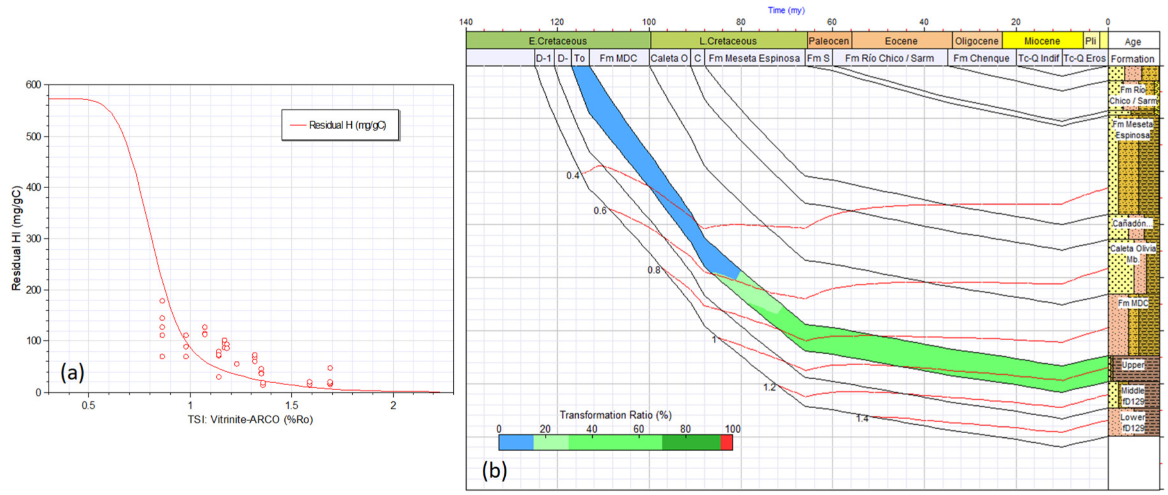

Figure 13. D129 Fm. 1D modeling in the well EH-307. (a) Kerogen kinetics simulation for the Hydrogen Index, circles: pyrolysis data, red curve: simulation.(b) Burial history and transformation ratio (%), red curves: simulated thermal maturity (VRE).

D129 Fm. Unconventional Play

The basic information presented in previous sections open the discussion to consider the D129 Fm. as an unconventional resource system giving entity to the Upper (a), Middle (b) and Lower (c) Sections. Figure 14 shows the corresponding isochore and thermal maturity maps (referred to "basement low thermal scenario").

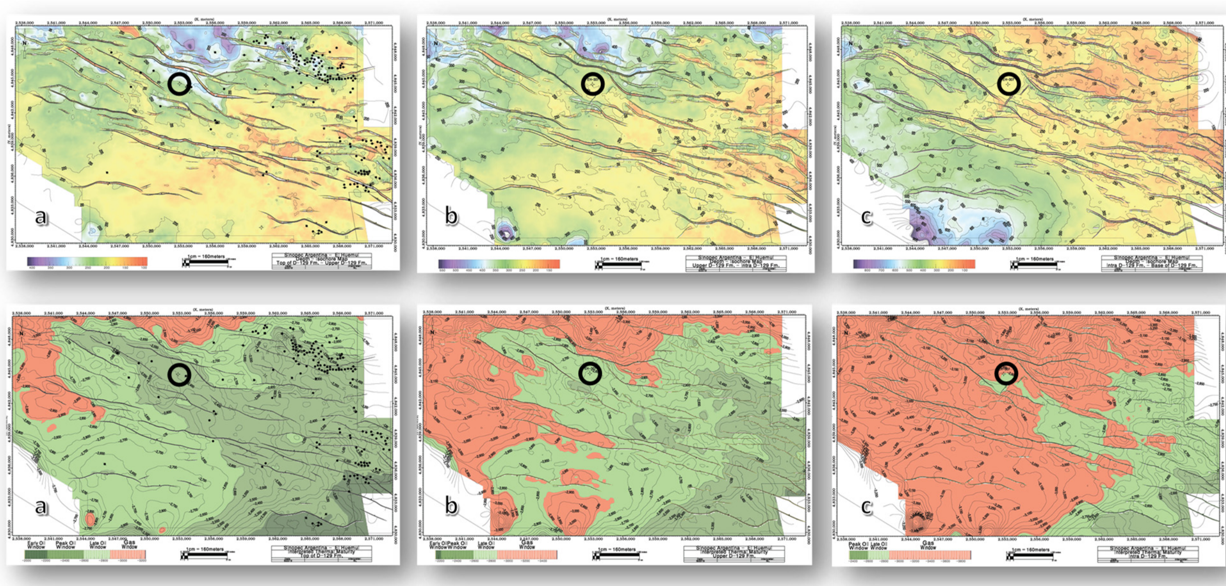

Figure 14. Above: D129 Fm. Isochore maps – (a) Upper Section – (b) Middle Section – (c) Lower Section // Wells reaching each section shown. Below: Thermal Maturity maps referred to "basement low scenario". // Location of well EH-307 circled.

D129 Fm. Upper Section

It is mainly composed by homogeneous black shales deposited under a lacustrine environment, in anoxic bottom water conditions, that accumulated a well-preserved organic matter with relatively homogeneous TOC all along the field, deriving in a Type I kerogen. The shallow paleoenvironmental position corresponding to well EH-307 as well as the "homogeneity" shown at this place on the lithological characteristics of this upper section, strongly reinforce the expected predominance of shale lithologies on its deeper (and less investigated) parts across EH Field. For most of the area, this section is within the oil generation window, where a shale oil play is then expected with a thickness ranging between 200 m and 300 m (Figure 14).

D129 Fm. Middle Section

Only drilled by well EH-307, its lithology is also dominated by black shales but with a frequent presence of interbedded permeable (lean) layers, in agreement with the associated shallower lacustrine depositional environment for this section. These alternations, mainly related to reworked tuffs and tuffaceous sandstones, might often constitute events of tight characteristics. Kerogen in the black shales is again well-preserved, although having a lower and more heterogeneous current TOC. In terms of maturity, this section will be within the late oil window for approximately half of the field, while the other half is expected to be in the gas window (Figure 14). This interbedding of shale and "tight" lithologies constitutes a *hybrid system* (Jarvie, 2012). Given the fact that the paleoenvironmental position of well EH-307 is representative for most of EH area, this system is then expected to be present along the largest portion of the field, possibly experiencing lateral variations of its "net-to-gross" relationship. Besides this, it could eventually make a transition into deeper lacustrine facies at the northern (central) region of the field because of the lower depositional environment that dominated this area. The system in the Middle Section has the potential to deliver around 250 m of vertical thickness of hydrocarbon target (oil or gas) but having particular characteristics. The organic-rich shale target combines with the interbedded reservoirs that may have underwent through direct hydrocarbon charging processes and, at the same time, could have the ability to act as "high permeability" drainage and production pathways (in relationship to the shaly background). Additionally, the potential of this system is reinforced by the rhythmic and frequent interbedding of shale and permeable lithologies.

D129 Fm. Lower Section

Drilled by EH-307, its lithology has a significant black shale participation but showing a more frequent interbedding of organic-lean layers (permeable) than the middle section. The kerogen is composed by a lower quality and less productive organic matter, according to samples from well EH-307. In terms of the thermal maturity, most of the section is expected to be in the gas window (Figure 14). The shallow paleoenvironmental position of EH-307 is representative of the north-eastern half of the field, with similar hybrid system characteristics than the Middle Section. In contrast, the south-western side is related to deeper paleoenvironmental conditions with a thicker Lower Section. This area may be subject to lower influence of the fluvial facies and, eventually, a transition into a shale target might take place.

Gathering the sections, D129 Fm. shows exceptional potential for unconventional hydrocarbon production. The Upper Section constitutes a shale-oil target having an average thickness of 250 m. Next, the Middle Section represents a hybrid system with the potential for oil and gas production. Last, the Lower Section potentially integrates two different unconventional targets having different potential and is expected to be within the gas window. When combined, these three sections represent an unconventional target that may have more than 700 m of vertical thickness in the oil window in certain areas while also potentially delivering 700 m of thickness in the gas window in other areas. This play having an unusually high thickness of source rock within the oil and gas windows is not only present under the 600 km^2 of areal extension of El Huemul Field, but it also has a natural occurrence under equivalent conditions on nearby fields. Furthermore, even when frequent reference is made to EH Field in this publication, regional data (partially shown in this publication) confirms the extension of this target over a basin level.

Fluid Characteristics

Liquid hydrocarbon fluids obtained from D129 Fm. in EH Field display significant differences with respect to produced oils in conventional reservoirs, which typically show variable degrees of biodegradation and mixing/rejuvenation processes, phenomenon that has been widely recognized at a basin scale (Philp, 1983; Villar *et al.*, 1996; Figari *et al.*, 1999, 2002; Jalfin *et al.*, 1999; Boll *et al.*, 2000; Villar *et al.*, 2000). In addition, D129 Fm. fluids also show dissimilar properties depending on whether they were obtained from the shale itself or from permeable levels within this formation, suggesting different source sections. These two hydrocarbon habitats are useful for target selection when combined with other parameters and can also be integrated with the processes that gave origin to CO_2 accumulations within D129 Fm. intervals.

Among others, well EHa-4301 (Figure 15) became archetypical to describe the nature of the hydrocarbons found in D129 Fm. in El Huemul Field, since it was the first one that received an unconventional fracture that targeted black shales in the Upper Section to produce a 43.3° API gravity light oil. The processing of open hole logs undoubtedly indicated dominant presence of shale lithologies and absence of permeable levels within the stimulated interval. Furthermore, geochemical assessments confirmed the occurrence of organic-rich beds (e.g. Figure 15a).

The chromatographic parameters of gas readings from mudlogging in well EHa-4301 are portrayed in Figure 15b. The application and interpretation of these relationships in the EH Field have been already discussed in detail by Jarque *et al.* (2019); therefore, only some outcomes will be mentioned here. Basically, the log shows the deepest section of the well and depicts at least three distinctive behaviors, two of them related to conventional targets. For Mina del Carmen Fm. (fMDC), the ratios predict the presence of light oil within reservoirs, consistent with the production tests. The plot also predicts the eventual presence of gas inside its background (fine) lithologies, which does not mean that gas could be produced, at least in the standard case. It is interpreted that, being non-permeable and organic-lean, these levels might only house small traces of light hydrocarbons, in line with the very low total gas readings from mudlogging. With regards specifically to the source rock section, the chromatographic ratios from gas readings suggest the presence of light oil inside the D129 Fm. black shales, in line with the late thermal maturity assessed for the stimulated interval of the well. The plot also depicts the increase in the total gas readings from mudlogging that is usual when entering D129 Fm. In terms of physical properties, shale oils associated to the late maturity window in the EH Field show API gravities at least 10° higher than conventional oils, which are in average less mature and have typically suffered in-reservoir alterations.

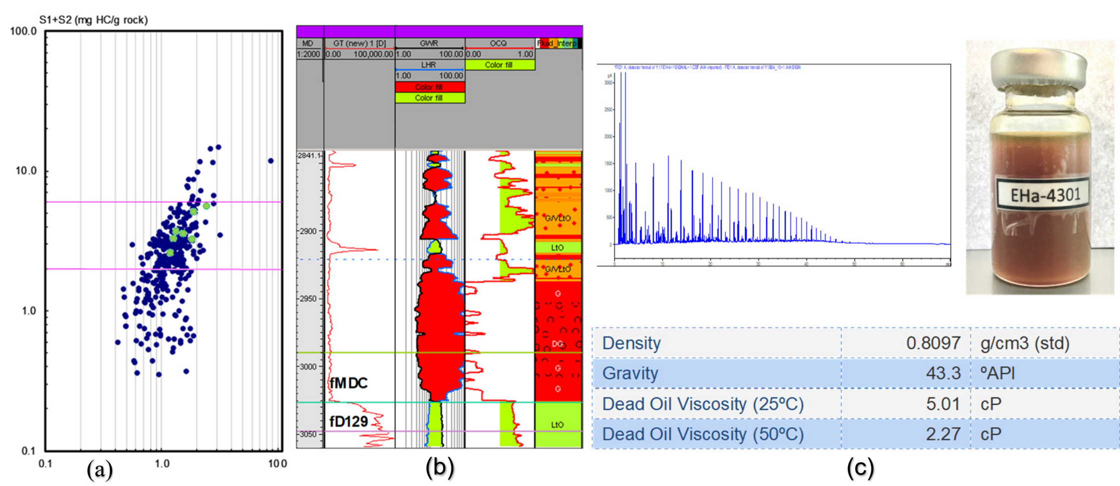

Figure 15. (a) (S1+S2) vs TOC of D129 Fm., with EHa-4301 data highlighted in green. (b) Chromatographic ratios applied to mudlogging readings (EHa-4301) (c) Gas chromatogram of D129 Fm. shale oil from EHa-4301 // Properties of shale oil sample (EHa-4301).

From the gas chromatography analysis of light hydrocarbons (LH), the EHa-4301oil shows a high n-heptane/cyclohexane ratio that points to a displacement along the thermal maturation vector in the typical plot of Thompson (1983) alterations diagram of Figure 16a. This high maturity trend is even more noticeable for the EH-4167 fluid, a 62.7º API gravity condensate recovered from a permeable, tuffaceous sandstone interval of D129 Fm. in the well. Other Thompson's parameters such as the Heptane and Isoheptane values are also consistent with a higher thermal maturity in EH-4167 with respect to EHa-4301. As expected, both samples present none of the typical alteration effects of water washing, biodegradation and evaporative fractionation that usually are identified for conventional-reservoired oils in the basin (some examples of El Huemul and neighbor areas are plotted in Figure 16a as reference). The D129 Fm. source pattern from LH of the EHa-4301oil is shown in the C Halpern (1995) star diagram of Figure 16b. An analogous pattern is recognized in the EH-4167 condensate, which points, as expected, to an origin from a nearby organic D129 Fm. facies. Allowing for degradation effects, a similar source is envisaged for the altered reference oils of conventional reservoirs. Similar conclusions are drawn from the evaluation of Mango (1994) LH parameters.

Bulk composition of both EHa-4301 (D129 Fm. shale oil) and EH-4167 (condensate lodged in permeable, non-shaly beds within D129 Fm.) samples are extremely enriched in saturated hydrocarbons (89.5-90.4%), a fact that is characteristic of high-mature, well preserved condensates and light oils. These data show a significant difference when compared to conventional oils depicted in Figure 16c because, with different degrees, all of them have been affected by complex histories of alteration (biodegradation) and rejuvenation thus resulting in averagely mid-mature oils that have moderate to significant participation of NSO and asphaltenes. Conversely, the condensate EH-4167 and the oil EHa-4301 are considered pristine fluids, in the sense that their genesis and accumulation within D129 Fm. intervals has prevented the biodegradation and mixing/rejuvenation processes that massively affected the conventional reservoirs of the basin.

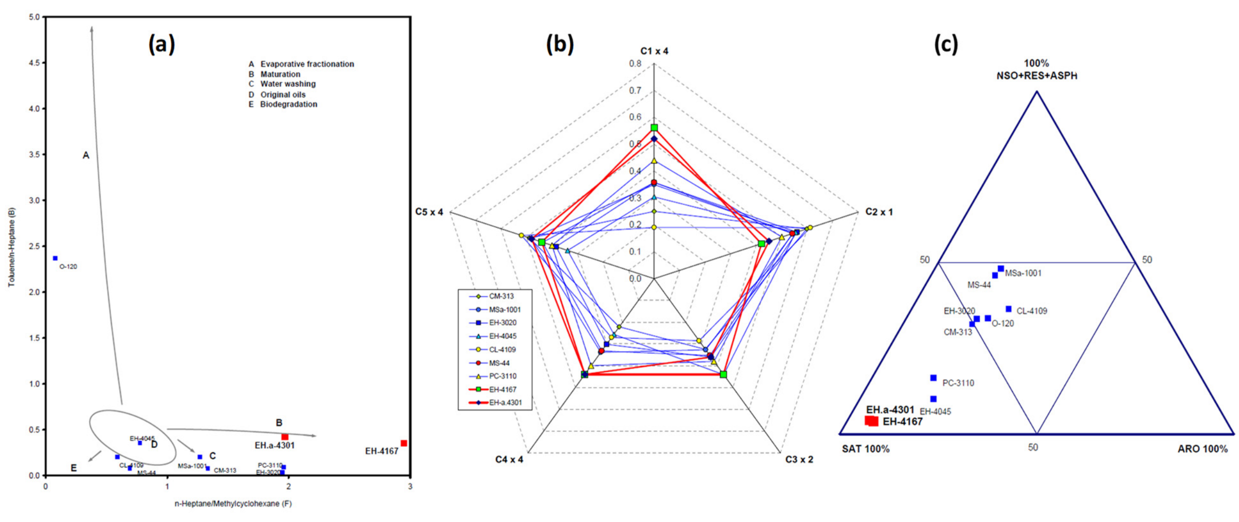

Figure 16. Oil and condensate analysis. (a) Thompson (1983) alteration vectors from light ends hydrocarbon data. (b) C Halpern (1995) plot from light hydrocarbon data. (c) Distribution of major compound groups from liquid chromatography data.

From biomarker fingerprints and LH patterns, the interpreted thermal maturity of the shale-oil EHa-4301 is consistent with an advanced stage of the oil window, reasonably in line with Ro measurements covering the range 1.05-1.16% in the associated D129 Fm. section. The thermal maturity attributed to the condensate EH-4167 is interpreted to be beyond the late oil window (VRE>1.3%) basically relying on LH data since biomarkers were marginally detected as traces and were not useful to calculate typical ratios, which is usual in high-maturity fluids. Shaly D129 Fm. beds close to the permeable reservoir interval yielded Ro measurements of 1.12-1.14%, strongly suggesting that the condensate EH-4167 represents a migrated fluid that was sourced from deeper and more mature D129 Fm. intervals. An additional piece of evidence to delineate these two habitats, that is, light oil in shales and very light condensate plus gas in permeable beds of D129 Fm., is given by the evaluation of chromatographic relationships (Jarque *et al.,* 2019) for well EH-4167 shown in Figure 17. The presence of locally generated light oil in the shale versus migrated and much lighter hydrocarbons in the permeable tuffaceous sandstone is a pattern not only recognized in wells EH-4167 and/or EHa-4301 but can be generalized for the D129 Fm. fluids through the EH Field. Thus, the use of chromatographic ratios becomes a predictive tool with the ability not only to differentiate shales from permeable levels but type of hydrocarbons as well.

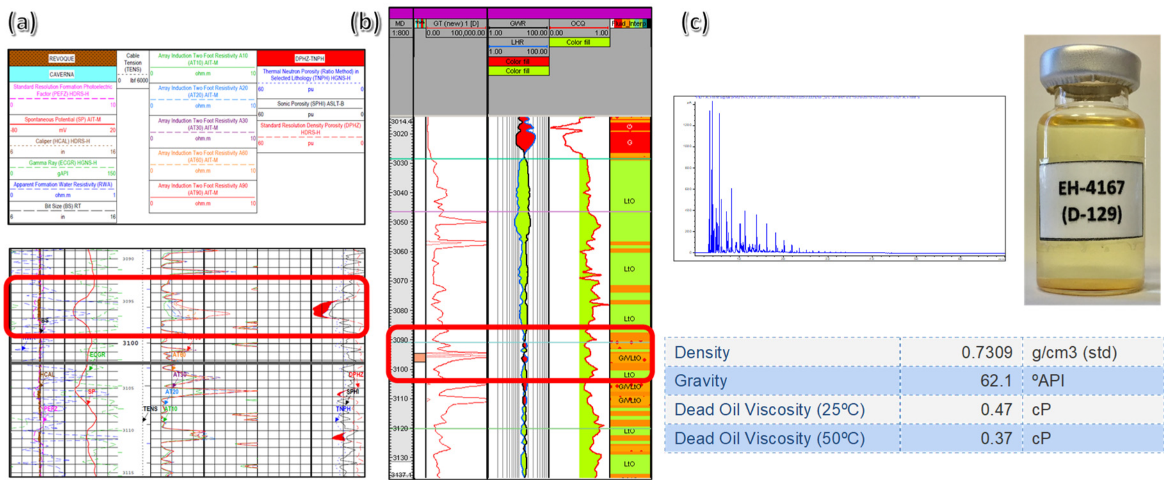

Figure 17. (a) EH-4167 OH Log highlighting open reservoir. (b) Chromatographic ratios applied to mudlogging readings (EH-4167) highlighting open reservoir. (c) Gas chromatogram of condensate from EH-4167 // Properties of the oil sample (EH-4167).

Supplementary indications of a deep and high-mature source feeding permeable beds within D129 Fm. in EH Field are documented by the carbon isotope signatures of two CO_2-rich (~90%) gas accumulations tested in permeable reservoir facies of well EH-4077. The $\delta^{13}C$ data of methane, ethane and propane of both gases indicate a very advanced post-maturity stage according to the inferred VRE of 1.8%. This thermal maturity is significantly greater than that indicated by Ro determinations for source rock levels of D129 Fm. that cover the range 0.93-1.22% in the well, implying mid to late stages of the oil window. It is worth to mention that the CO_2 origin of these accumulations has been assessed to be of magmatic origin as revealed by the composition and isotopic analyses of carbon dioxide and noble gases. To present date, the shale play of D129 Fm. has always been tested to have a very low CO_2 content along the EH Field, fact that is consistent with a migrated magmatic source, since the intrinsic petrophysical properties would impose a strong restriction to the hypothetical charge and accumulation of this gas in the shale.

Conclusions

The appraisal of the D129 Fm. looking for unconventional opportunities in El Huemul Field (EH) led to a shale oil discovery in well EHa-4301 within typical lacustrine source rock facies. This well tested oil during completion and continued to produce under regular field operations. This and other wells allowed to demonstrate that black shales belonging to D129 Fm. can be fractured and that its hydrocarbons accumulations have the ability to flow, thus reinforcing the productive potential of this unconventional play.

Geochemical analysis in the EH Field and neighbor areas (411 cutting samples from 19 wells) points out to the presence of high quality, oil-prone Type I kerogen in the organic richest lacustrine facies that showed HI values close to 600 mg HC/g TOC for the marginal to early mature positions, while enrichment with Type III kerogen should be expected in the transition into terrestrial facies. Most of the samples of D129 Fm. collected in the EH Field showed mid to advanced thermal maturity, and therefore, a significant decrease in the original HI values in line with substantial conversion to hydrocarbons.

The first hydrocarbon fluids produced from the D129 Fm. unconventional play have revealed no alteration evidence, contrary to the oils produced from the conventional reservoirs that typically show variable degrees of biodegradation, rejuvenation and mixing processes that involve renewed migration pulses. In addition, accumulations within the D129 Fm. present different patterns depending on whether they are hosted in the shale itself or in permeable levels. The in-shale reservoired fluid represents a light-oil that has been generated by the local source rock, while the fluid produced from permeable lithologies (typically tuffaceous sandstones) represents a migrated, very light oil condensate assumed to be sourced from deeper and more mature D129 Fm. beds. In particular, the produced shale oil exhibits an API gravity around 44º that reflects an outstanding quality in comparison with the average conventional hydrocarbons of the basin.

The shale play of D129 Fm. has been tested to have a very low content of CO_2 across the EH Field. In contrast, higher CO_2 amounts have always been found related to accumulations present in permeable levels, and a dominantly magmatic origin has been assessed. The occurrence of reservoirs very rich in CO_2 (up to around 90%) depends on the availability to connect the reservoirs to the magmatic source of the CO_2. Therefore, the understanding of the migration processes that led to CO_2 accumulations in the permeable levels of D129 Fm. is relevant to limit CO_2 production during exploration and development stages of this unconventional play.

The unconventional potential of the D129 Fm. remains outstanding:

- The D129 Fm. Upper Section constitutes a shale-oil target of 250 m thick in the mid to late oil window. Migrated very light condensates in permeable beds, mostly tuffaceous sandstones, conform an additional target.
- The D129 Fm. Middle Section represents a hybrid system with potential for hydrocarbons in the late oil and gas-condensate thermal maturity windows.
- The D129 Fm. Lower Section integrates a high maturity unconventional target within the gas window.

When combined, these three sections represent an unconventional resource system that may surpass *700 m of vertical thickness for both liquid and gas hydrocarbons* depending on the thermal maturity throughout an extended area of 600 km^2 in the EH Field. Moreover, analogous unconventional plays are expected to be present in nearby fields of the South Flank of the basin.

Acknowledgement

The authors want to express their gratitude to the authorities of Sinopec Argentina Exploration and Production Inc. for the permission to publish the information included in this paper. Special thanks are also given to Rodrigo Rodriguez and Eduardo Figari for the recommendations made after reading this manuscript.

References

Archangelsky, S., and J. Seiler, 1980, Algunos resultados palinológicos de la perforación UN Oil OS-1, del SO de la Provincia del Chubut, Argentina: II Congreso Argentino de Paleontología y Bioestratigrafía, 5, p. 215-225.

Basile, Y.A., S.M. Utgé, V. Martínez Cal, and C. Ponce, 2014, Avances en el conocimiento sobre la capacidad generadora de la Fm Pozo D-129: aspectos litológicos y geoquímicos. Cuenca del Golfo San Jorge, Argentina: IX Congreso de Exploración y Desarrollo de Hidrocarburos, IAPG, p. 265-285.

Boll, A., L. Chelotti, G. Laffitte, and H.J. Villar, 2000, Petroleum habitat in the El Tordillo Field and adjacent areas, North Flank of the Golfo San Jorge Basin, Argentina: different opportunities for oil and gas emplacement, *in* L.A.F. Trindade, A.C. Macedo and S.M. Barbanti, eds., Proceedings Seventh Latinamerican Congress on Organic Geochemistry, Foz do Iguaçu, Brazil, Oct. 22-26, 2000 p. 305-307.

Clavijo, R, 1986, Estratigrafía del Cretácico Inferior en el sector occidental de la Cuenca Golfo San Jorge: Boletín de Informaciones Petroleras, Año III, 9, p. 15-32.

Dingle, R.V., W.G. Siesser, and A.R. Newton, 1983, Mesozoic and Tertiary Geology of Southern Africa: A.A. Balkema, Rotterdam, 375 p.

Figari, E., M. Cid De La Paz, and G. Laffite, 1997, Modelos de hemigrábenes en el Neocomiano del sector occidental de la Cuenca del Golfo San Jorge, Argentina: sistemas petroleros, origen e inversión tectónica: Boletín de Informaciones Petroleras, 52, p. 5-17.

Figari, E.G., E. Strelkov, , G. Laffitte, M.S, Cid de la Paz, S.F. Courtade, J. Celaya, A. Vottero, P. Lafourcade, R. Martínez, and H.J. Villar, 1999, Los sistemas petroleros de la Cuenca del Golfo San Jorge. Síntesis estructural, estratigráfica y Geoquímica: Actas I, IV Congreso de Exploración y Desarrollo de Hidrocarburos, IAPG, p. 197-237

Figari, E.G., E. Strelkov, M.S, Cid de la Paz, G. Laffitte, and H.J. Villar, 2002, Cuenca del Golfo San Jorge: síntesis estructural, estratigráfica y geoquímica, *in* M.J. Halle ed., Geología y Recursos Naturales de Santa Cruz. Relatorio del XV Congreso Geológico Argentino, III-1, AGA, p. 571-601.

Figari, E.G., and D.G. García, 2018, Modelos analógicos superficie subsuelo para el Chubutiano Inferior de las Cuencas de Cañadón Asfalto y del Golfo San Jorge, Argentina: X Congreso de Exploración y Desarrollo de Hidrocarburos, IAPG, p. 669-688.

Figari, E.G., J.J. Hechem, M.J. Continanzia, A. Gavarrino, N. Urrez, and D.G. García, 2020, Cuencas Hidrocarburíferas, sus Sistemas Petroleros y Principales Yacimientos. Relatorio XXI Congreso Geológico Argentino (in press).

Fitzgerald, M., R. Mitchum, M.A. Uliana, and K. Biddle, K, 1990, Evolution of the San Jorge Basin. AAPG Bulletin, v. 74, p. 879-920.

Halpern, H. I., 1995, Development and applications of light-hydrocarbon-based star diagrams: AAPG Bulletin, v. 79, p. 801-815.

Hechem, J. J., and E. Strelkov, 2002, Secuencia sedimentaria Mesozoica del Golfo San Jorge. *in* M.J. Halle ed., Geología y Recursos Naturales de Santa Cruz. Relatorio del XV Congreso Geológico Argentino v.1, p. 129-147.

Jalfin, G., E. Bellosi, J. Sanagua, and H. J. Villar, 1999, Procesos múltiples de migración, alteración y mezcla en petróleos de la Cuenca del Golfo San Jorge: una evaluación geoquímica integrada: IV Congreso de Exploración y Desarrollo de Hidrocarburos, IAPG, p. 445-465.

Jarque, G., G. Maiztegui, P. Caprioglio, A. D'Agostino, N. Luz, and M. Irigoyen, 2019, Relaciones cromatográficas aplicadas al desarrollo no convencional de la Formación Pozo D-129. Yacimiento El Huemul, Cuenca del Golfo San Jorge: VII Congreso de Producción y Desarrollo de Reservas, pendrive IAPG, 21p.

Jarvie, D. M., 2012, Shale resource systems for oil and gas: Part 2—Shale-oil resource systems, in J. A. Breyer, ed., Shale reservoirs—Giant resources for the 21st century: AAPG Memoir 97, p. 89–119.

Legarreta, L., and H.J. Villar, 2011, Argentina basins: Geological and geochemical keys of the potential shale resources: AAPG Geoscience Technology Workshop, "Unconventional Resources: Basics, Challenges, and Opportunities for New Frontier Plays," Buenos Aires, Argentina, 26–28 June, accessed

June 12, 2019, http://www.searchanddiscovery.com/pdfz/documents/2011/ 80196legarreta/ ndx_legarreta.pdf.html.

Lesta, P, 1968, Estratigrafía de la Cuenca del Golfo San Jorge: *Actas III Jornadas Geológicas Argentinas*, 1, p. 251-289.

Mango, F. D., 1994, The origin of light hydrocarbons in petroleum: Ring preference in the closure of carbocyclic rings: Geochimica et Cosmochimica Acta, v. 58, p. 895–901.

Paredes, J. M., N. Foix, F. Colombo Piñol, A. Nillni, J.O. Allard, and R.A. Marquillas, 2007, Volcanic and climatic controls on fluvial style in a high-energy system: The Lower Cretaceous Matasiete Formation, Golfo San Jorge Basin, Argentina: Sedimentary Geology, v. 202, p. 96-123.

Pepper, A. S., and P.J, Corvi, 1995, Simple kinetic models of petroleum formation. Part 1: oil and gas generation from kerogen: *Marine and Petroleum Geology*. v. 12, p. 291-319.

Philp R.P., 1983, Correlation of crude oils from the San Jorges Basin, Argentina: Geochimica et Cosmochimica Acta, v. 47 (2), p. 267-275.

Rodríguez, J. F. R., and R. Littke, 2001, Petroleum generation and accumulation in the Golfo San Jorge Basin, Argentina: a basin modeling study: Marine and Petroleum Geology, v. 18, p. 995-1028.

Stach, H., and A. Ansa, 2014, Regional seismic interpretation on Pozo D-129 Formation in the South Flank of the Golfo San Jorge Basin, SINOPEC Internal Report.

Sylwan, C.A., J,F, Rodríguez, and E.E. Strelkov, 2008, Petroleum systems of the Golfo San Jorge Basin, Argentina, *in* C.E. Cruz, J.F. Rodríguez, J.J. Hechem and H.J. Villar eds., Simposio de Sistemas Petroleros de las Cuencas Andinas, VII Congreso de Exploración y Desarrollo de Hidrocarburos, IAPG, Buenos Aires, p. 53-77.

Thompson, K. F. M., 1983, Classification and thermal history of petroleum based on light hydrocarbons: Geochimica et Cosmochimica Acta, v. 47, p. 303–316.

Uliana, M., L. Legarreta, G. Laffitte, and H.J. Villar, 1999, Estratigrafía y geoquímica de las facies generadoras de hidrocarburos en las cuencas petrolíferas de Argentina: Actas I, IV Congreso de Exploración y Desarrollo de Hidrocarburos, IAPG, p. 1-61.

Urien, C., J. Zambrano, and L. Martins, 1981, The basins of southeastern South America (southern Brazil, Uruguay and eastern Argentina) including the Malvinas Plateau and the southern South Atlantic paleogeographic evolution, *in* W.Volkheimer and E. Musacchio, eds., Cuencas Sedimentarias del Jurásico y Cretácico de América del Sur, I, Buenos Aires, p. 45-125.

Utgé, S., S. Martinez Cal, Y. Basile, and C. Ponce, 2014, Evaluación del potencial de la Formación Pozo D-129 como reservorio no convencional shale gas/oil. IX Congreso de Exploración y Desarrollo de Hidrocarburos, Simposio de Recursos No Convencionales, IAPG, p. 117-135.

Van Nieuwenhuise, D. S., and A.R. Ormiston,1989, A model for the origin of source-rich lacustrian facies, San Jorge Basin, Argentina: 1° Congreso de Exploración y Producción de Hidrocarburos, IAP, II, p. 853-883.

Villar, H.J., C.A. Sylwan, A. Gutiérrez Pleimling, M. Miller, J.R. Castaño, and W.G, Dow, 1996, Formación de petróleos pesados a partir de procesos de biodegradación y mezcla en el sistema petrolero Pozo D-129 -Cañadón Seco, Flanco Sur de la Cuenca del Golfo San Jorge, Santa Cruz, Argentina: III Congreso de Exploración de Hidrocarburos, v. 1, p. 223-243.

Villar, H.J., G. Jalfin, E.S. Bellosi, and G.A. Laffitte, 2000, Oil biodegradation in the Golfo San Jorge Basin, Argentina, *in* L.A.F. Trindade, A.C. Macedo and S.M. Barbanti, eds., Proceedings Seventh Latinamerican Congress on Organic Geochemistry, Foz do Iguaçu, Brazil, Oct. 22-26, 2000, p. 17-19.

Yllañez, E. D., J.P. Di Lena, and H.G. Marchese, 1989, Evaluación geoquímica de petróleos y rocas generadoras en la Cuenca del Golfo San Jorge, Argentina: 1° Congreso de Exploración y Producción de Hidrocarburos, IAP, II, p. 1127-1157.